Expression of the Minor Isoform Pea Ferredoxin in Tobacco Alters Photosynthetic Electron Partitioning and Enhances Cyclic Electron Flow[1][W]

Nicolás E. Blanco*, Romina D. Ceccoli, María V. Dalla Vía, Ingo Voss, María E. Segretin, Fernando F. Bravo-Almonacid, Michael Melzer, Mohammad-Reza Hajirezaei, Renate Scheibe, and Guy T. Hanke

Umeå Plant Science Centre, Department of Plant Physiology, Umeå University, SE 901 87 Umea, Sweden (N.E.B.); Instituto de Biología Molecular y Celular de Rosario (Consejo Nacional de Investigaciones Científicas y Técnicas), División Biología Molecular, Facultad de Ciencias Bioquímicas y Farmacéuticas, Universidad Nacional de Rosario, S2002LRK Rosario, Argentina (R.D.C.); Instituto de Investigaciones en Ingeniería Genética y Biología Molecular (Consejo Nacional de Investigaciones Científicas y Técnicas), Laboratorio de Virología y Biotecnología Vegetal, C1428ADN Ciudad Autónoma de Buenos Aires, Argentina (M.V.D.V., M.E.S., F.F.B.-A.); Pflanzenphysiologie, Fakultät Biologie/Chemie, Universität Osnabrück, D–49069 Osnabrueck, Germany (I.V., R.S., G.T.H.); and Leibniz-Institut für Pflanzengenetik und Kulturpflanzenforschung, Physiologie und Zellbiologie, 06466 Gatersleben, Germany (M.M., M.-R.H.)

Ferredoxins (Fds) are ferrosulfoproteins that function as low-potential electron carriers in plants. The Fd family is composed of several isoforms that share high sequence homology but differ in functional characteristics. In leaves, at least two isoforms conduct linear and cyclic photosynthetic electron transport around photosystem I, and mounting evidence suggests the existence of at least partial division of duties between these isoforms. To evaluate the contribution of different kinds of Fds to the control of electron fluxes along the photosynthetic electron transport chain, we overexpressed a minor pea (*Pisum sativum*) Fd isoform (PsFd1) in tobacco (*Nicotiana tabacum*) plants. The transplastomic *OeFd1* plants exhibited variegated leaves and retarded growth and developmental rates. Photosynthetic studies of these plants indicated a reduction in carbon dioxide assimilation rates, photosystem II photochemistry, and linear electron flow. However, the plants showed an increase in nonphotochemical quenching, better control of excitation pressure at photosystem II, and no evidence of photoinhibition, implying a better dynamic regulation to remove excess energy from the photosynthetic electron transport chain. Finally, analysis of P700 redox status during illumination confirmed that the minor pea Fd isoform promotes enhanced cyclic flow around photosystem I. The two novel features of this work are: (1) that Fd levels achieved in transplastomic plants promote an alternative electron partitioning even under greenhouse light growth conditions, a situation that is exacerbated at higher light intensity measurements; and (2) that an alternative, minor Fd isoform has been overexpressed in plants, giving new evidence of labor division among Fd isoforms.

During photosynthesis, the outward electron flow from PSI leads to the reduction of ferredoxin (Fd), a soluble electron shuttle containing a [2Fe-2S] iron-sulfur cluster center as its prosthetic group (Hase et al., 2006). The main use for these photosynthetic electrons is the generation of the NADPH needed for carbon dioxide (CO_2) assimilation, which is accomplished through reoxidation of Fd in a reaction catalyzed by Fd-$NADP^+$ reductase (FNR; Ceccarelli et al., 2004; Mulo, 2011). The transfer of electrons from water to $NADP^+$ is the principal mechanism of linear electron flow (LEF) and is one of the possible fates of electrons moving through the photosynthetic electron transport chain (PETC). Alternatively, Fd may return electrons to the plastoquinone (PQ) pool of the PETC, mediating a cyclic flow around PSI (CEF-PSI; Shikanai, 2007; Rochaix, 2011). This alternative route of electron donation by Fd is also coupled to the generation of a transthylakoid proton gradient (ΔpH) to (1) produce additional ATP with no net reduction of $NADP^+$ and (2) induce the dissipative mechanisms of nonphotochemical quenching (NPQ), which help maintain the redox poise of the PETC (Munekage et al., 2004; DalCorso et al., 2008). CEF-PSI can proceed through two partially redundant pathways, either the Fd-dependent route involving a putative

[1] This work was supported by a grant from the Deutscher Akademischer Austauschdienst, Germany, and DFG-Sachbeihilfe Grant HA 5921/1–1. M.E.S. and F.F.B.-A. are staff members and R.D.C. and M.V.D.V. are fellows from Consejo Nacional de Investigaciones Científicas y Técnicas.

* Corresponding author; e-mail nicolas.blanco@plantphys.umu.se.
The author responsible for distribution of materials integral to the findings presented in this article in accordance with the policy described in the Instructions for Authors (www.plantphysiol.org) is: Nicolás E. Blanco (nicolas.blanco@plantphys.umu.se).

[W] The online version of this article contains Web-only data.
www.plantphysiol.org/cgi/doi/10.1104/pp.112.211078

Fd-quinone reductase and the PROTON GRADIENT REGULATION5/PGR5-LIKE PHOTOSYNTHETIC PHENOTYPE1 (PGR5/PGRL1) complex and/or via the membrane-bound NADPH dehydrogenase complex (NDH; Munekage et al., 2004; DalCorso et al., 2008). Besides these two divergent electron flow routes, Fd is also the low-potential electron donor to many metabolic and regulatory pathways of the chloroplast. They include nitrogen and sulfur assimilation, fatty acid desaturation, regeneration of peroxiredoxin and ascorbate, and reduction of thioredoxin via Fd-thioredoxin reductase (Schürmann and Buchanan, 2008). Therefore, Fd plays a dual role in primary and secondary metabolism, as donor of reducing equivalents and at the same time as a regulatory component of the activation state of key enzymes associated with these metabolisms.

Higher-plant Fds are encoded by a small gene family, with distinct isoforms present in chloroplasts and nonphotosynthetic plastids (Hanke et al., 2004; Hanke and Hase, 2008; Voss et al., 2008, 2011). Chloroplasts from C3 plants contain at least two isoforms that accumulate to different levels and share a high degree of sequence identity (Hanke et al., 2004). In recent years, a suite of publications has reported novel insights into the functionality of specific isoforms and their influence on plastid and plant metabolism (Kimata-Ariga et al., 2000; Hanke et al., 2004; Hanke and Hase, 2008; Voss et al., 2008, 2011).

Kimata-Ariga et al. (2000) have reported that the expression of a particular isoform from a C4 plant (bundle sheath cell-specific Fd II from maize [*Zea mays*]) enhances CEF-PSI to the detriment of NADPH production and nitrogen assimilation in cyanobacterium (Kimata-Ariga et al., 2000). In this case, the authors identified an amino acid difference that lead to decreased interaction with FNR and stimulated CEF. However, this difference is not conserved with any other reported Fd amino acid sequence. Indeed, analysis of Fd isoproteins indicates that sequence identity is often higher between photosynthetic isoforms of the same species, relative to orthologs of closely related genera (Hanke and Hase 2008; Blanco et al., 2011, Supplemental Fig. S1). A thorough comparison of the biochemical properties of two photosynthetic Fds from the same species has only been performed with proteins from pea (*Pisum sativum*; Dutton and Rogers, 1980) and Arabidopsis (*Arabidopsis thaliana*; Hanke et al., 2004). In both cases, only minor differences were detected in redox potential, electron transfer capacity with FNR, and $NADP^+$ photoreduction, indicating that there must be significant redundant capacity and yielding no information on any molecular mechanism that could be responsible for differential electron partitioning.

Nevertheless, in both Arabidopsis and pea, abundance of the two Fd isoproteins varies dramatically. For example, in Arabidopsis, AtFd1 and AtFd2 represent about 10% and 90% of the total photosynthetic Fd pool, respectively (Hanke et al., 2004), and under low growth light, pea leaves express mainly PsFd2, while PsFd1 cannot be detected (Khristin and Akulova, 1976; Peltier et al., 2000). However, under conditions thought to stimulate CEF, such as drought or high light, transcripts of AtFd1, but not AtFd2 increase significantly (Lehtimäki et al., 2010), while PsFd1 becomes the most abundant isoprotein in pea leaves (Khristin and Akulova, 1976). Moreover, studies conducted with both knockout and knocked-down (RNA interference [RNAi]) Arabidopsis plants have suggested that the minor AtFd1 isoform might be primarily engaged in CEF-PSI, whereas AtFd2 is mainly responsible for LEF, although some redundancy in these functions has also been observed (Hanke and Hase, 2008; Voss et al., 2008). Knockout and RNAi plants deficient in AtFd2 displayed lower electron transport rates (ETRs), an overreduced PETC, and growth penalties linked to lower CO_2 assimilation, whereas AtFd1-deficient lines showed minor phenotypic changes and an enhanced LEF under certain circumstances.

Complementary to these knockout and knockdown studies, it would be of great value to analyze plants in which the different kinds of photosynthetic Fd isoprotein were overexpressed. Until now, the only work concerning this issue has been the expression of the major Arabidopsis isoprotein, AtFd2, in tobacco (*Nicotiana tabacum*) chloroplasts using a transplastomic strategy. The transgenic plants obtained did not show a dramatic phenotype, and the CEF-PSI was enhanced only at high-light growth intensities (Yamamoto et al., 2006). However, no attempt has yet been made to overexpress one of the minor Fd isoproteins, which have been proposed to differentially operate in CEF.

To gain a better comprehension of this aspect of plant biology, we generated transplastomic tobacco plants expressing the minor Fd isoform from pea (PsFd1). Unexpectedly, the transgenic plants exhibited a range of abnormalities, including moderate growth retardation, a leaf-variegated phenotype, and impaired photosynthesis. Electron transport measurements revealed that the transformants had elevated CEF-PSI, which was accompanied with a reduction in LEF, resulting in lower carbon assimilation rates and a significant increase in the NPQ mechanism. The results strongly support the notion that specific chloroplast Fd isoforms are evolutionarily tailored to produce alternative electron partitioning between linear and cyclic electron flow.

RESULTS

Preparation and Characterization of *OeFd1* Plants

Two different Fd isoforms could be detected in protein extracts from pea leaves, with a minor isoform (PsFd1) accounting for about 6% of the total Fd pool, assuming equal antigenicity (Fig. 1A, lane 1). Using the reported coding sequence of PsFd1 (accession no. M31713; Supplemental Fig. S1), we engineered tobacco plants by direct chloroplast transformation (Maliga, 2004) with the plasmid pBSWutr-PsFd1 (see "Materials and Methods"). The transgene was inserted by homologous

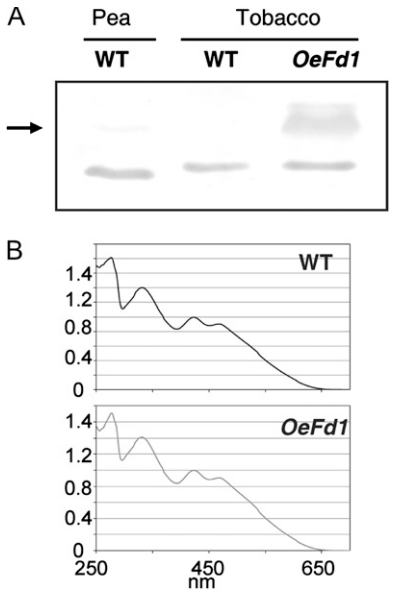

Figure 1. Functional Fd isoform accumulation in 8-week-old tobacco and pea plants. Fd isoforms in leaf extracts of wild-type (WT; lane 2) and *OeFd1* (lane 3) tobacco and wild-type pea (lane 1) plants were resolved using SDS-PAGE and immunoblotting (A). Protein extracts corresponding to 0.45 mg of leaf fresh weight were loaded in each lane. Electrophoretic mobility of the minor pea Fd is indicated by an arrow. Spectrum of purified PsFd1 protein isolated from leaves of *OeFd1* showing correct assembly of prosthetic group [2Fe2S] (B).

recombination at a single locus of the plastid genome, and homoplasmic lines (*OeFd1*) were isolated by successive rounds of in vitro regeneration under selection (Supplemental Fig. S2). To evaluate transgene expression, protein extracts from leaves of *OeFd1* and wild-type plants were resolved by SDS-PAGE and blotted onto nitrocellulose membranes. Detection of PsFd1 was carried out using polyclonal antisera raised against recombinant PsFd1, which also reacted with the endogenous orthologs (Blanco et al., 2011). An extra immunoreactive band was detected in *OeFd1* plants (Fig. 1A, lane 3). It showed lower electrophoretic mobility relative to the endogenous tobacco Fds and comigrated with the minor Fd protein identified in pea leaf extracts (Fig. 1A, lane 1). As previously reported, independent transgenic specimens did not show position effects (Daniell et al., 2002; Blanco et al., 2011; Ceccoli et al., 2012), and all transplastomic lines obtained showed similar phenotypic characteristics (Supplemental Fig. S2) and yielded essentially the same PsFd1 contents in leaves of homoplasmic lines. Quantification of the various Fd species based on scanning of individual immunoreactive bands and comparison with pure standards indicates that *OeFd1* plants accumulated 5.76 ± 0.46 μmol PsFd1 m^{-2} and 3.20 ± 0.74 μmol m^{-2} of endogenous Fd, whereas wild-type plants contained 2.96 ± 0.54 μmol Fd m^{-2}. Therefore, the expression of tobacco Fds does not appear to be affected by accumulation of the foreign iron-sulfur protein. To complete the initial characterization of the transgenic lines, we confirmed that the introduced PsFd1 protein was folded into its functional form on expression in tobacco chloroplasts. The Fd fraction of leaves from both wild-type and *OeFd1* plants was purified, and both show the characteristic absorption spectrum of a plant type [2Fe-2S] Fd, with a functionally assembled prosthetic group (Fig. 1B). The yield of purified Fd was approximately 4 times greater from transplastomic than from wild-type plant leaves (46 mg and 8.2 mg per kg fresh weight, respectively), indicating that the introduced Fd is correctly assembled into the holoform. In addition, the spectra of the two Fd fractions show subtle differences around the peak at 280 nm, reflecting differences in aromatic amino acid side chains between Fd from wild-type tobacco, and Fd isolated from *OeFd1* plants, which contain a high proportion of the introduced pea Fd1.

Surprisingly, the transformed lines showed growth retardation, as evidenced by delayed flowering and lower biomass accumulation, lower number of nodes, and shorter internodal distance, and exhibited variegated leaves through all stages of their lifetime (Fig. 2; Table I). Analysis of photosynthetic pigments in whole leaves revealed that 9-week-old *OeFd1* plants contained approximately 17% less total chlorophyll with respect to wild-type siblings, with no modifications in the chlorophyll *a*/*b* ratio and carotenoid contents (Table I). To further characterize the nature of the variegated phenotype of *OeFd1* plants, leaf cross sections of the wild type and *OeFd1* were analyzed by light microscopy and transmission electron microscopy (TEM). Histological analysis under the light microscope shows differences in the distribution of chloroplasts in the palisade parenchyma (PP) cells (Fig. 3, A–D). While chloroplasts in wild-type PP revealed regular distribution of chloroplasts on the anticlinal and the inner periclinal cell walls (Fig. 3, A and B), PP cells of *OeFd1* plants were characterized by an accumulation of chloroplasts at the inner periclinal cell walls (Fig. 3, C and D). Compared with the wild type, TEM images of *OeFd1* cells show numerous vesicles in the central vacuole and the chloroplasts displayed less starch granules. Plastids of *OeFd1* plants contained a higher number of plastoglobuli and swollen grana thylakoids, indicating a disarrangement of the membranes throughout the cell (Fig. 3, E–G and H–J).

Chlorophyll Fluorescence Parameters in *OeFd1* Plants

The characteristics displayed by *OeFd1* plants contrast with those reported by Yamamoto et al. (2006), who observed no significant phenotypic alterations in transplastomic tobacco plants expressing the major Fd isoprotein of Arabidopsis, AtFd2, which is known to be predominantly involved in LEF. Indeed, many of the features observed in *OeFd1* lines actually resembled those normally exhibited by Fd-deficient (antisense or silenced) plants (Holtgrefe et al., 2003; Blanco et al., 2011), although the levels of endogenous tobacco Fd were not affected in *OeFd1* lines (Fig. 1A), ruling out any negative feedback regulation between alien

Figure 2. Impact of Fd overexpression on plant growth, development, and leaf morphology. Phenotype of 4-week-old wild-type (left) and *OeFd1* (right) plants growing on Murashige and Skoog-0 (A). Phenotype of 6-week-old wild-type (left) and *OeFd1* (right) plants growing on soil (B). Phenotype of 11-week-old wild-type (left) and *OeFd1* (right) plants growing on soil (C). Image of third fully expanded leaf belonging to wild-type and *OeFd1* plants (D). Insets show variegation in *OeFd1* leaves.

and endogenous isoforms. To investigate the physiological basis for these phenotypic effects, the functionality of the PETC was evaluated by chlorophyll fluorescence measurements under steady-state conditions. Relative to wild-type siblings, dark-adapted *OeFd1* plants displayed slightly lower maximum quantum yield values of PSII (maximum photochemical efficiency of PSII in the dark-adapted state [F_v/F_m]), concomitant with an increase in initial (minimum) PSII fluorescence in the dark-adapted state (F_0; Table II; Fig. 4). When assayed at growth light intensity (200 μmol quanta m^{-2} s^{-1}), the maximum photochemical efficiency of PSII during steady-state illumination (F_v'/F_m') and the operating efficiency [Φ_{PSII} or Y (PSII)] were decreased compared with wild-type plants, suggesting a smaller fraction of absorbed excitation energy was converted by PSII in photochemistry and LEF. In addition, the NPQ parameter did not differ significantly in this measurement at steady-state conditions (Table II). One possible cause of the differences between wild-type and *OeFd1* tobacco might be altered stoichiometry of the components of the PETC chain, and we therefore compared the abundance of components of PSII, complex Cytb_6f, and PSI by western blotting (Fig. 5). These blots showed no significant difference between the genotypes, suggesting that the measured differences in chlorophyll fluorescence parameters are due to other indirect effects (such as thylakoid membrane rearrangement and/or variegation), rather than direct changes to the stoichiometry of the main components of the PETC. Another possible cause of increased F_0 in the *OeFd1* plants could be incomplete relaxation of ΔpH during the dark preincubation of plants. To establish if this was the case, we repeated our measurements following overnight dark incubation and found that the F_0 values of dark-adapted *OeFd1* plants remained higher than the control (*OeFd1*, F_0 = 0.608 ± 0.038, maximum PSII fluorescence in the

Table I. *Determination of phenotypic parameters in PsFd1-overexpressing and wild-type tobacco plants*

Plants were grown on soil for 9 weeks in a growth chamber under the conditions described in "Materials and Methods." Experimental procedures to determine pigments are also given there. Values reported are means ± SD of seven individual plants. Asterisks indicate significant differences between *OeFd1* and wild-type (WT) plants with $P < 0.05$ (*) or $P < 0.005$ (**).

Phenotypic and Biochemical Parameters	WT	*OeFd1*
No. of Nodes	11.14 ± 0.90	9.41 ± 1.12**
Height (cm)	76.71 ± 8.83	46.80 ± 15.81**
Internodal distance (cm)	4.71 ± 0.39	4.00 ± 0.43**
Aerial fresh weight (g)	84.93 ± 13.69	66.86 ± 20.76*
Aerial dry weight (g)	5.72 ± 1.01	4.10 ± 1.74*
Water (%)	93.30 ± 0.50	93.93 ± 1.23
Chlorophyll *a* (μg cm^{-2})	21.18 ± 1.55	17.44 ± 2.68**
Chlorophyll *b* (μg cm^{-2})	6.77 ± 0.43	5.77 ± 0.48**
Total chlorophyll (μg cm^{-2})	27.96 ± 1.72	23.21 ± 3.08**
Carotenoids (μg cm^{-2})	4.97 ± 0.45	4.66 ± 0.94
Chlorophyll *a*/chlorophyll *b*	3.12 ± 0.25	3.02 ± 0.31
ATP/ADP	1.00 ± 0.04	1.25 ± 0.06**

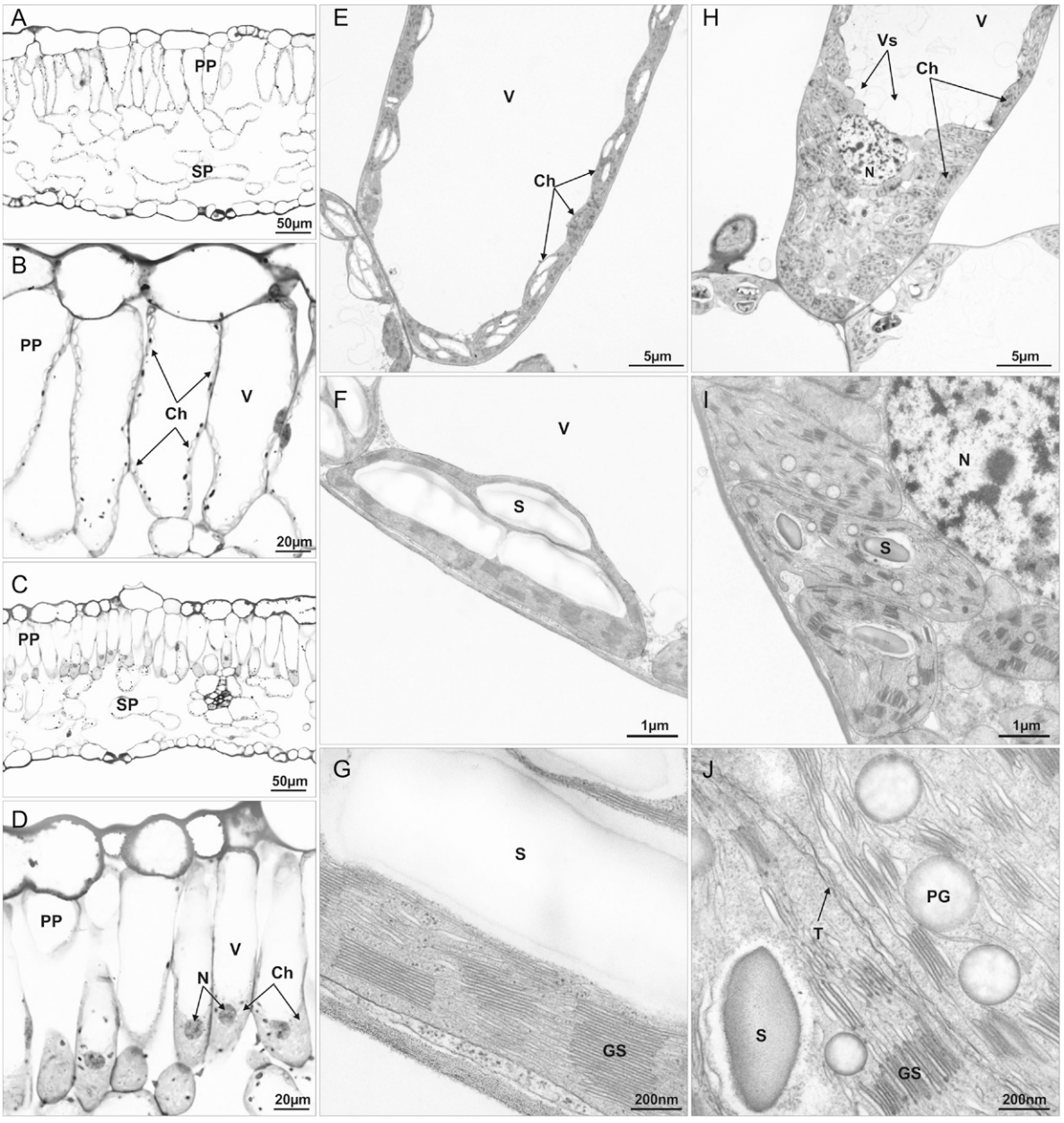

Figure 3. Light microscopy and TEM of leaf tissue of wild-type and *OeFd1* plants. Light microscopy (A–D) and TEM (E–J) of cross sections of source leaves of wild-type (A, B, and E–G) and *OeFd1* plants (C, D, and H–J). PP of wild-type plants shows regular distribution of the chloroplasts on the anticlinal and the inner periclinal cell walls (A, B, and E), while cells of *OeFd1* plants were characterized by an accumulation of chloroplasts at the inner periclinal cell walls (C, D, and H). In contrast with the wild type, vacuoles of *OeFd1* plants contain numerous vesicles (E and H) and chloroplasts show less starch granules, a higher number of plastoglobuli, and swollen grana thylakoids (E–J). Ch, Chloroplast; GS, grana stack; N, nucleus; PG, plastoglobuli; S, starch; SP, spongy parenchyma; T, thylakoid; V, vacuole; Vs, vesicle.

dark-adapted state [F_m] = 2.053 ± 0.133; the wild type, F_0 = 0.405 ± 0.047, F_m = 2.133 ± 0.130).

Similar measurements were carried out on specimens grown under standard greenhouse conditions but using 1000 μmol quanta m^{-2} s^{-1} as measuring actinic light (AL). Under these conditions, the PSII photochemistry of transgenic plants remained below the values observed in wild-type plants, with lower F_v'/F_m', Φ_{PSII}, and carbon assimilation rates (A_{CO2}; Table II). Unlike photochemical parameters, the NPQ value was markedly increased in *OeFd1* plants (Table II). The chlorophyll fluorescence steady-state values and traces collected at both light intensities (Table II; Fig. 4; Supplemental Fig. S3), plus the higher F_0 values of dark-adapted *OeFd1* plants, suggest that although the transgenic line is less photochemically

Table II. *Determination of chlorophyll fluorescence parameters in PsFd1-overexpressing and wild-type tobacco plants*

Nine-week-old plants were measured 3 to 6 h into the light period and dark incubated for 30 min prior to dark-adapted measurements (F_v/F_m). Light-adapted determinations were performed after 30 min of exposure to 200 and 1000 μmol quanta m^{-2} s^{-1}. Data reported are means ± SD of at least six measurements on independent plants. Asterisks indicate significant differences between *OeFd1* and wild-type (WT) plants with $P < 0.05$ (*) or $P < 0.005$ (**).

Chlorophyll Fluorescence and Photosynthetic Parameters	WT	*OeFd1*	WT	*OeFd1*
	200 μmol quanta m^{-2} s^{-1}		1000 μmol quanta m^{-2} s^{-1}	
F_v/F_m	0.808 ± 0.005	0.693 ± 0.019**	0.781 ± 0.014	0.686 ± 0.012**
F_0	0.389 ± 0.006	0.592 ± 0.065**	0.429 ± 0.020	0.569 ± 0.062**
F_m	2.027 ± 0,039	1.954 ± 0.052*	1.955 ± 0.045	1.807 ± 0.057*
F_v'/F_m'	0.750 ± 0.003	0.602 ± 0.023**	0.479 ± 0.004	0.347 ± 0.010**
Φ_{PSII}	0.710 ± 0.005	0.585 ± 0.047**	0.186 ± 0.013	0.167 ± 0.011*
NPQ	0.227 ± 0.007	0.197 ± 0.027*	1.839 ± 0.059	2.434 ± 0.081**
A_{CO2} (μmol CO_2 m^{-2} s^{-1})	7.96 ± 0.35	6.93 ± 0.41**	10.22 ± 0.30	8.22 ± 0.54**

efficient than the wild type, it is not disproportionally affected by increasing light intensity.

To exclude any adaptive processes that could be triggered by HL during steady-state measurements, we used a shorter measuring time scale to estimate CO_2 assimilation rates, ETR, and NPQ values. The transformants showed lower CO_2 assimilation rates and ETR (Fig. 6, A and B) relative to wild-type siblings at all tested light intensities, whereas NPQ exhibited a relatively large increase to 500 μmol quanta m^{-2} s^{-1} (Fig. 6C). The differential photosynthetic performance in *OeFd1* plants was independent of the developmental stage as it was also observed in measurements conducted on older plants (Supplemental Fig. S4).

One explanation for the decreased photochemistry of *OeFd1* plants and its high F_0 values might be increased photoinhibition of PSII, even though levels of PsbA (D1) indicate this is not the case (Fig. 5; Edelman and Mattoo, 2008). To gain further insight into possible photoinhibition in the *OeFd1* plants, we measured the partitioning or fate of absorbed excitation energy into two extra components besides Φ_{PSII} [also named as Y(PSII), Y (NO), and Y(NPQ); Klughammer and Schreiber, 2008]. The measurements of these three parameters under AL at growth light intensity are shown in Table III. In comparison with wild-type plants, *OeFd1* plants presented an alternative partitioning of the absorbed energy, with a decrease in the fraction of energy that is photochemically converted at PSII [Y(PSII)] as a consequence of higher heat dissipation via the regulated photoprotective NPQ mechanism [Y(NPQ)]. Furthermore, these plants did not exhibit a concomitant rise in Y(NO), which is equivalent to the fraction of energy passively dissipated mainly as consequence of closed PSII reaction centers (RCs). This last value is in line with the *qL* parameter, which is a complementary indicator of openness of the PSII RC (Baker, 2008).

Taken together, the whole data set indicate that *OeFd1* plants are not photoinhibited and that the ratios between components of the different CET complexes are relatively unchanged apart from Fd complement but that partitioning of energy around the PETC system is altered compared with the wild type. While they display a decreased LEF, the higher Fd content seems to favor nonassimilative processes (NPQ), which might help in part to relieve excitation pressure over the PETC at increasing light intensities.

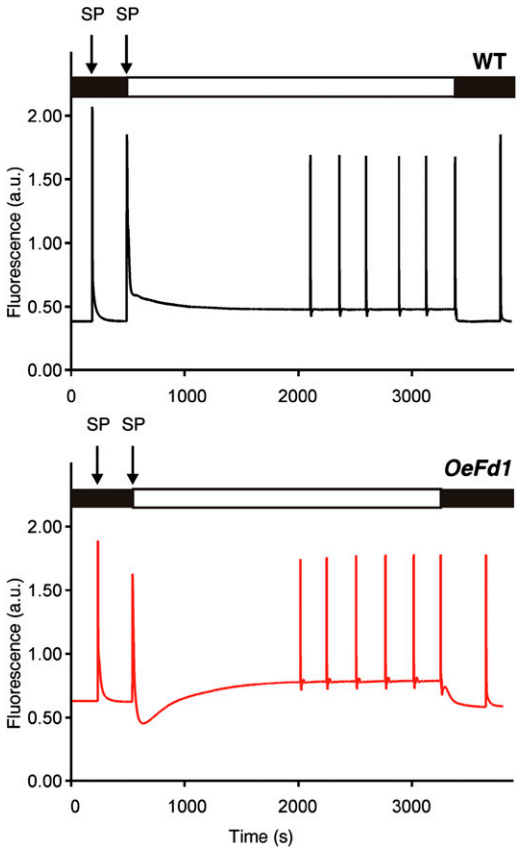

Figure 4. Fluorescence traces in *OeFd1* and wild-type (WT) plants under steady-state conditions. Typical chlorophyll fluorescence traces in a dark-adapted leaf of wild-type (top curve) and *OeFd1* plants (below curve) under illumination with standard AL (200 μmol quanta m^{-2} s^{-1}) are shown. Black and white boxes above the traces indicate absence and presence of AL illumination. Arrows mark the application of the first two saturating pulses. The traces belong to representative curves from nine independent experiments for each line. a.u., Arbitrary units.

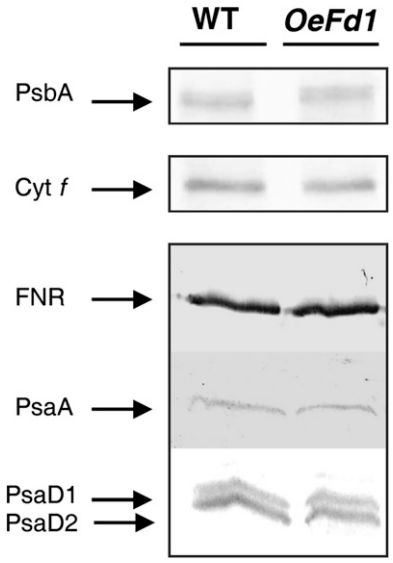

Figure 5. PSII, complex Cytb_6f, and PSI proteins in wild-type (WT) and *OeFd1* total leaf extracts. Proteins from total leaf extracts were separated by SDS-PAGE and immunoblotted onto nitrocellulose membranes. Total leaf extracts were used to detect PsbA (5 μg of protein), Cyt*f* (20 μg of protein), and FNR (20 μg of protein). PsaD1 and PsaD2 were detected on soluble extracts containing 20 μg of protein in each line.

Evidence for Elevated CEF-PSI Activity in *OeFd1* Plants

Since NPQ largely relies on the generation of a ΔpH, through electron movement in the PETC, and LEF was decreased in *OeFd1* plants, we evaluated the hypothesis that alternative electron partitioning could favor CEF-PSI in PsFd1-overexpressing plants. One way to monitor electron donation from stromal reductants to the PQ pool is by measuring chlorophyll fluorescence during light-dark transitions (Burrows et al., 1998; Kofer et al., 1998; Sazanov et al., 1998; Shikanai et al., 1998). Figure 7 shows typical results obtained with wild-type and *OeFd1* plants adapted for 30 min to 200 or 1,000 μmol quanta m^{-2} s^{-1}. Both lines displayed a typical transient rise in chlorophyll fluorescence after turning off AL, which increased at elevated light intensities (Fig. 7B). However, the magnitude of the dark response was higher in *OeFd1* plants than in the wild type. It is worth noting that the chlorophyll fluorescence dark relaxation signal of *OeFd1* plants exposed to 1000 μmol quanta m^{-2} s^{-1} increased above that observed at 200 μmol quanta m^{-2} (Fig. 7) and that during dark relaxation, *OeFd1* fluorescence levels exceeded those seen during illumination (Fig. 7B; Supplemental Fig. S3). The increased NPQ in *OeFd1* under these conditions (Fig. 6) presumably contributes to the decreased chlorophyll fluorescence signal and the enhanced dark relaxation.

To obtain a better understanding of the PsFd1-dependent changes that might produce a higher electron flow into the PQ pool, we measured the redox status of PSI by monitoring the absorbance changes at 830 nm. Near infrared (NIR) illumination was used to preferentially oxidize the PSI RC, and the rate of dark rereduction was estimated after turning off the NIR light (Ivanov et al., 2006). The maximum P700 oxidation value ($\Delta P700_{max}$) was 40% lower in *OeFd1* plants (Fig. 8A, left panel; Table IV), and the rate of $P700^+$ dark reduction also showed altered kinetics. Analysis of this process on attached leaves of wild-type and *OeFd1* plants indicated a faster reduction step in PsFd1-overexpressing plants, which fitted a double exponential decay function (Fig. 8B, continuous-line traces; Table IV). The calculated $\tau_{1/2}$ for the first phase of the exponential decay in *OeFd1* leaves was 3- to 4-fold faster than that of the wild type, and the second component was also slightly faster (Table IV). Faster rereduction of the primary electron donor of PSI ($P700^+$) in *OeFd1* plants could be caused by either an increase in electron donation to PSI, likely via enhanced CEF-PSI or an impairment of electron output. No differences between wild-type and *OeFd1* plants could be

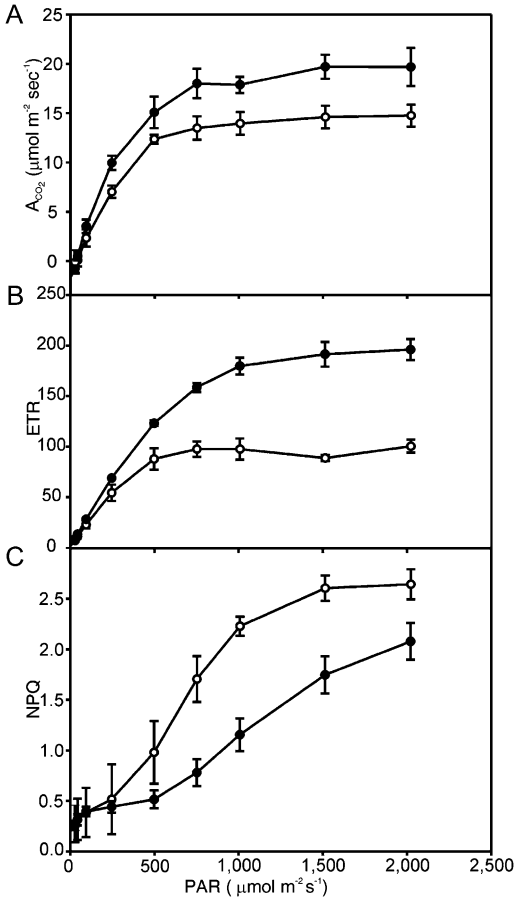

Figure 6. *OeFd1* plants have lower CO_2 assimilation activity and ETR as well as enhanced NPQ induction. Light response curves of net photosynthetic rates corresponding to 8-week-old wild-type (black circles) and *OeFd1* (white circles) leaves (A). Determinations were carried out on the second and third youngest fully expanded leaves. Fluorescence determinations to obtain ETR (B) and NPQ (C) were run in parallel with CO_2 assimilation rate data collection. In all cases, each data point represents the average ± SE of five assays on independent plants. PAR, Photosynthetically active radiation.

Table III. *Quantum yield of PSII photochemistry and associated parameters under growth light intensity in leaves from PsFd1-overexpressing and wild-type tobacco plants*

Nine-week-old plants were assayed 3 to 6 h into the light period and dark adapted for 30 min prior to measurements. Data reported are means ± SD of at least 10 measurements on independent plants. Asterisks indicate significant differences between *OeFd1* and wild-type (WT) plants with $P < 0.05$ (*) or $P < 0.005$ (**).

PSII Photochemistry-Associated Parameters	WT	*OeFd1*
Y(PSII)/Φ_{PSII}	0.619 ± 0.022	0.374 ± 0.030**
Y(NO)	0.256 ± 0.029	0.217 ± 0.017*
Y(NPQ)	0.125 ± 0.032	0.409 ± 0.011**
qL	0.387 ± 0.010	0.572 ± 0.037**

detected at the protein level for FNR, PsaA, PsaD, Cyt*f*, or PsbA (Fig. 5), strongly suggesting that the effects observed did not result from alterations in the stoichiometry of the PSI complex or between the different components of the PETC. We repeated the P700 measurements after infiltration with 50 μM 2,5-dibromo-6-isopropyl-3-methyl-1,4-benzoquinone (DBMIB). This compound binds to the Q_o pocket of the cytochrome b_6f complex and competes with PQ (Roberts and Kramer, 2001), preventing reduction of the complex. Table IV, Figure 8, and Supplemental Figure S5 show that, for both evaluated parameters ($\Delta P700_{max}$ and $P700^+$ reduction $\tau_{1/2}$), the effect of DBMIB was more substantial on *OeFd1* leaves than on wild-type leaves. Following DBMIB infiltration, *OeFd1* showed an approximately 28% increase in $\Delta P700_{max}$ with respect to water-treated plants, whereas wild-type plants showed little or no difference.

To further characterize the activity of PSI in *OeFd1* plants, we used AL (200 and 1000 μmol quanta m^{-2} s^{-1}) instead of NIR to record the redox turnover of P700 under conditions in which both photosystems are operating. The oxidation kinetics of P700 by AL in wild-type plants showed two phase kinetics, with a very rapid initial oxidation followed by reduction and then a slower increase in oxidation. *OeFd1* plants also showed this two-phase kinetics, but the rate of oxidation for both phases was much slower, indicating either less efficient oxidation or more efficient rereduction of PSI (Supplemental Fig. S6).

We subsequently adapted the previous experiment to leaf discs to improve uptake of the inhibitors of PETC employed to probe CEF-PSI functionality. Using water as a vacuum infiltration control yielded only minor differences in the oxidation kinetics of PSI in this experimental system (Fig. 9A). Leaf discs were infiltrated with methyl viologen (MV), which is a more efficient electron acceptor than any Fd isoform and should therefore function as the main PSI oxidant by AL. Exposure to 100 μM MV led to similar P700 oxidation curves in both wild-type and *OeFd1* plants (Fig. 9B). These results indicate that electron output from PSI before donation to Fd was not compromised in *OeFd1* plants and that PsFd1 is at least partially responsible for the observed difference in electron distribution. To determine whether the slow oxidation of P700 in *OeFd1* plants is due to electron transport from the PQ pool, rather than inefficient oxidation of PSI by Fd or electron backflow from soluble acceptors directly to PSI, measurements were also made in the presence of 50 μM DBMIB. Once again, both wild-type and *OeFd1* plants showed the same pattern of P700 oxidation (Fig. 9C). Collectively, these results demonstrate that (1) the differential oxidation pattern of *OeFd1* PSI by AL was not linked to alterations in PSI itself (Fig. 5), and (2) the most likely cause of these slower oxidation kinetics originates in enhanced electron flow from the stromal pool back into the PETC via the cytochrome b_6f complex.

Due to increased ΔpH formation, enhanced CEF-PSI also is expected to enhance ATP production (Shikanai, 2007). In accordance with this presumption, the ATP/ADP ratio of *OeFd1* plants was found to be 20% higher relative to the wild type (Table I), lending further support to the notion that CEF-PSI activity was exaggerated in *OeFd1* plants. Taken together, these observations allow us to conclude that expression in tobacco of the minor, alternative pea Fd isoform, PsFd1 introduced significant changes in photosynthetic electron partitioning and that these are consistent with CEF-PSI being favored over LEF.

DISCUSSION

Overexpression of PsFd1 in Tobacco Plants Results in a Dramatic Phenotypic Effect

Since the discovery that several Fd isoforms are present in leaf chloroplasts, a critical question has been whether these various forms can differentially partition electrons to either LEF or CEF-PSI (Hanke et al., 2004; Hanke and Hase, 2008; Voss et al., 2008). Although some

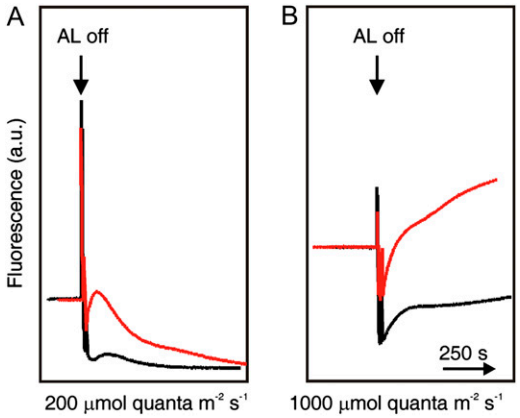

Figure 7. Comparison of postillumination fluorescence rise in wild-type and *OeFd1* plants. The fluorescence postillumination rise was recorded after 30 min of AL illumination with 200 (A) and 1,000 (B) μmol quanta m^{-2} s^{-1} in wild-type (black traces) and *OeFd1* (red traces) leaves. AL off arrows indicate the cessation of AL illumination. Representative traces are from at least six independent experiments for each line and each treatment. a.u., Arbitrary units.

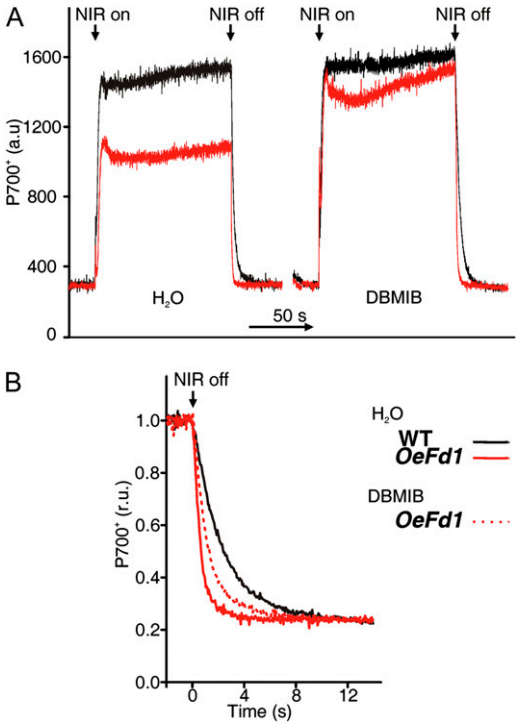

Figure 8. Comparison of P700 oxidation by NIR light on whole leaves in 9-week-old wild-type and *OeFd1* plants. The top panel shows typical time courses for wild-type plants (black traces) with the upward/downward arrows indicating NIR treatment frame (A). As above, black and red curves correspond to wild-type and *OeFd1* leaves. Bottom panel corresponds to scaling up and normalization to units of PSI reduction induced by turning off NIR illumination (B). Traces in dotted lines correspond to the same experiment with *OeFd1* leaves previously infiltrated with 50 μM DBMIB. a.u., Arbitrary units; WT, the wild type.

degree of functional redundancy clearly exists based on work with purified proteins (Dutton and Rogers, 1980; Hanke et al., 2004), genetic evidence points to differential electron partitioning and suggests a predominant role for the more abundant of the two Fd isoforms in LEF and greater involvement of the minor isoform in CEF (Yamamoto et al., 2006; Hanke and Hase, 2008; Voss et al., 2008). For instance, tobacco plants transformed with AtFd2 did not show an obvious phenotype and only exhibited an increase in CEF-PSI at HL growth intensities and low partial pressures of oxygen, conditions in which photorespiration was suppressed (Yamamoto et al., 2006). To date, only the more abundant cyanobacterial or higher plant Fds have been overexpressed in plants, resulting in no dramatic phenotypic effect (Yamamoto et al., 2006; Ceccoli et al., 2011). To gain greater understanding of Fd functional diversity, we investigated whether an alternative, low abundance, higher plant Fd isoprotein might promote alternative electron transport pathways by introducing the minor pea Fd isoform (PsFd1) into tobacco plants and characterizing the phenotype and photosynthetic activity of the resulting transgenic plants (*OeFd1* lines).

In contrast with studies in which major Fd isoforms were overexpressed (Yamamoto et al., 2006; Ceccoli et al., 2011), the expression of this alternative, minor leaf-type Fd did have phenotypic consequences in the resulting transformants, causing moderate growth retardation, a decrease in chlorophyll contents without changes in carotenoid levels, and variegated leaves throughout the entire life cycle of the plant (Table I; Fig. 2). Some of these features resembled those displayed by plants in which chloroplast Fds have been knocked down by antisense or RNAi strategies (Holtgrefe et al., 2003; Blanco et al., 2011), raising the possibility that expression of endogenous Fds could be repressed in *OeFd1* lines. Cross-regulation of Fd expression has previously been observed in a number of cases (Hanke and Hase, 2008; Voss et al., 2011). However, this hypothesis was ruled out for *OeFd1* lines by western-blot Fd quantification, in which the density of the total tobacco Fd pool was not impacted by expression of PsFd1 in *OeFd1* plants (Fig. 1A). It is likely that introduction of the PsFd1 transgene into the plastid genome allowed its expression to bypass the nuclear-cytosolic regulatory constraints that usually affect Fd mRNA levels (Petracek et al., 1998; Ceccoli et al., 2011). Retarded growth of *OeFd1* plants is consistent with lower CO_2 assimilation, relative to the wild type, at all light intensities assayed (Table II; Fig. 6; Supplemental Fig. S4), pointing to a decreased efficiency of PETC and photosynthetic performance as a possible cause of the phenotype.

OeFd1 Plants Have Decreased LEF and an Increase in NPQ Mechanism

Although no change was detected in the relative abundance of protein components of the PETC, analysis of PSII function revealed several alterations in electron

Table IV. *Kinetics of P700 turnover under NIR illumination in leaves from PsFd1-overexpressing and wild-type tobacco plants*

Nine-week-old plants were assayed 3 to 6 h into the light period and dark adapted for 30 min prior to measurements. Data reported are means ± SD of at least 10 measurements on independent plants. Asterisks indicate significant differences between *OeFd1* and wild-type (WT) plants with $P < 0.005$ (**).

P700 Parameters	WT	*OeFd1*	WT	*OeFd1*
	H_2O		DBMIB	
$\Delta P700_{max}$	1,259.3 ± 72.5	793.8 ± 92.9**	1,288.9 ± 70.2	1,101.8 ± 88.3**
$\tau_{1/2}$ (1st phase, s^{-1})	1.53 ± 0.22	0.43 ± 0.05**	2.07 ± 0.26	0.69 ± 0.11**
$\tau_{1/2}$ (2nd phase, s^{-1})	6.53 ± 1.52	2.75 ± 0.53**	4.35 ± 1.46	3.41 ± 0.25

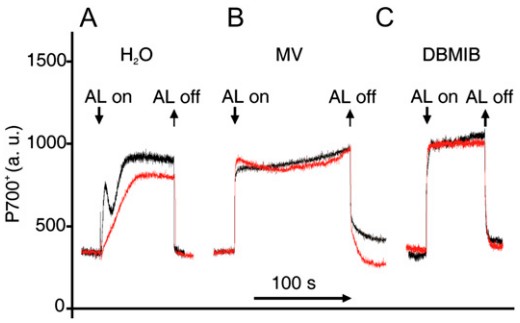

Figure 9. Effect of PETC inhibitors on differential P700 oxidation kinetics by AL. Comparison of P700 oxidation by AL in leaf discs of wild-type (black traces) and *OeFd1* (red traces) plants. Discs were vacuum infiltrated with water (A), 100 μM MV (B), or 25 μM DBMIB (C) by 30 s and then dark adapted for at least 15 min. Arrow meanings are equal to previous figures.

distribution through the chain. The ability to perform photochemistry was diminished in *OeFd1* lines, as indicated by both steady-state and rapid measurements, although higher light intensity did not significantly increase these problems relative to the wild type (Tables II and III; Figs. 4 and 6; Supplemental Figs. S3 and S4). The decrease in LEF rate was accompanied by a slower reopening of RCs after the first saturation pulse (SP) and a decrease of chlorophyll fluorescence below the F_0 level after the second SP and the start of AL (Table II; Fig. 4; Supplemental Fig. S3). These abnormalities in chlorophyll fluorescence using the SP method, and more precisely during the dark-light transition, plus the high values of F_o and the lower Φ_{PSII}/Y(PSII) could be interpreted as a signature of photoinhibition. However, we found no significant change in the PsaB subunit of PSII, indicating that this protein, and PSII in general, are probably not disproportionally degraded in *OeFd1* plants (Edelman and Mattoo, 2008). Although *OeFd1* plants did have a decreased Y(PSII) at the beginning of illumination with normal growth AL after dark adaptation (Table II), when the fate of absorbed energy at PSII was examined (as outlined in Klughammer and Schreiber, 2008), we found that an increased efficiency of NPQ appeared to be responsible for this less efficient photochemistry in *OeFd1* (Table III). Moreover, the *qL* parameter showed the PSII RC was actually more open, indicating a more oxidized state of the first acceptor (Q_A), and the fraction of energy passively dissipated in the form of heat or fluorescence [Y(NO)] was similar between wild-type and *OeFd1* plants. These results clearly argue against a simple saturation of the PETC or an extensive photoinhibitory process (Shikanai et al., 1999; Baker, 2008).

This apparently paradoxical behavior of *OeFd1* plants, i.e. a larger electron acceptor pool with a significant decrease in LEF and no signs of photoinhibition, is accompanied by a greater capacity to cope with HL intensities by deploying an augmented NPQ response, even at older developmental stages (Table II; Fig. 6; Supplemental Fig. S4). Fd-dependent NPQ is involved in the dissipation of excess energy and is governed by the extent of the proton gradient generated across the thylakoid membranes, as modulated by CEF-PSI (Müller et al., 2001; Munekage et al., 2004; Shikanai, 2007; DalCorso et al., 2008). In an analogous rationale to the screen for mutants with defects in CEF (Shikanai et al., 1999), the most likely explanation for these results is that, when expressed in tobacco chloroplasts, the minor PsFd1 isoform favors alternative partitioning of electrons into CEF-PSI over LEF.

The Expression of *PsFd1* Leads to an Alternative Partitioning, Favoring CEF

Based on current dogma, the most likely reason for the altered electron partitioning in the *OeFd1* plants is an enhanced CEF. Although no definitive method is available to measure this phenomenon, we used several indirect techniques, which all gave results consistent with enhanced CEF. An enhanced CEF-PSI mediated by PsFd1 is consistent with the transient rise in chlorophyll fluorescence exhibited by *OeFd1* plants after turning off AL (Fig. 7). This phenomenon has been attributed to PQ reduction by stromal reductants via NDH (Burrows et al., 1998; Kofer et al., 1998; Sazanov et al., 1998; Shikanai et al., 1998). The identification of a novel component of the NDH complex, named CRR31, whose predicted tertiary structure shares common aspects with PsaE Fd-docking site, strongly suggests direct electron transfer from Fd to this complex and, therefore, a direct contribution of Fd to the increased transient rise in fluorescence (Yamamoto et al., 2011). Moreover, the participation of Fd in this post-illumination increase in fluorescence has recently been reported (Gotoh et al., 2010). Therefore, the contribution of excess Fd-dependent CEF in *OeFd1* lines may be sufficient to explain this difference (Fig. 7). Considering all these variables, the enhanced CEF in *OeFd1* transplastomic plants might provide the electron flow required to sustain an energetic-dependent NPQ rise, which in turn relaxes after turning off AL (Shikanai, 2007). Moreover, the NDH-dependent CEF pathway has been shown to be responsible for dark-dependent input of electrons to PETC (Sazanov et al., 1998), and enhancement of this process could in part help to explain the increased F_0 values measured in *OeFd1* plants following dark adaptation. Analysis of P700 turnover also provided support for the hypothesis that CEF-PSI activity was exaggerated in PsFd1-expressing lines. The combination of lower $\Delta P700_{max}$ and higher $P700^+$ reduction rates, as illustrated in Figure 8, Supplemental Figure S5, and Table IV, has been linked to increased CEF-PSI both in vivo and in vitro (Ivanov et al., 2006; Iwai et al., 2010; Lehtimäki et al., 2010). We detected no significant modifications in extrinsic and intrinsic protein components of PSI, PSII, and complex Cytb_6f (Fig. 5), indicating that the altered photochemistry of *OeFd1* plants was not caused by changes in PSI composition or in other components of

PETC. Results obtained using NIR illumination could be reproduced on exposure to AL, under conditions in which both photosystems are expected to function (Fig. 9). In agreement with previous reports (Endo et al., 2005; Joliot and Joliot, 2005), use of inhibitors such as DBMIB and MV confirmed that the lower $\Delta P700_{max}$ of *OeFd1* lines was caused by faster $P700^+$ reduction rather than a deficiency in electron removal from PSI (Table IV; Figs. 8 and 9).

We therefore propose a model, in which at the levels of expression obtained in *OeFd1* plants (approximately 2- to 4-fold over endogenous Fd forms), PsFd1 competes with native tobacco Fd for reducing equivalents generated at the PETC and delivers them preferentially to CEF-PSI instead of LEF. Our analysis indicates that the phenotype of the *OeFd1* plants is partly due to competitive inhibition of LEF, caused by PsFd1 requisitioning electrons for CEF. Theoretically, such inhibition might be overcome by increasing light intensities, as more electrons become available for CO_2 fixation. However, our data clearly show that the lower values of A_{CO2} and ETR seen in the *OeFd1* plants (Fig. 6; Supplemental Fig. S4) are saturated and cannot be overcome by increasing light intensities. Clearly, another factor, apart from electron partitioning away from CO_2 fixation, is limiting electron flux in the transplastomic plants. We propose that this is an inhibition of the PET chain by overacidification of the lumen. Enhanced CEF in the *OeFd1* plants would lead to a more rapid acidification of the thylakoid lumen, which is known to inhibit activity of the complex Cytb_6f in particular (Kramer et al., 1999). We therefore suggest that CO_2 fixation rates are limited by lower ETR through the thylakoid membrane complexes in *OeFd1* plants, caused by inhibition of the Cytb_6f at lower pH values generated by the exaggerated CEF conducted by PsFd1. In this way, enhanced CEF could actually result in growth retardation, emphasizing the importance of regulating the abundance of specific Fd isoforms in the native plant. Indeed, it has been reported that Fd1 massively increases in abundance in pea leaves at higher light intensities, consistent with a physiological need for up-regulated CEF (Khristin and Akulova, 1976).

Genetic evidence, including that provided here, strongly supports a model in which Fd1 and Fd2 differentially partition electrons. However, previous studies on purified proteins from both pea and Arabidopsis have failed to find any significant differences between the redox potential or electron transfer activities of two alternative photosynthetic Fds from the same species (Dutton and Rogers, 1980; Hanke et al., 2004). Moreover, intraspecies homology of Fd1 and Fd2 is often greater than interspecies homology (Hanke and Hase, 2008), complicating the identification of Fd1 or Fd2 specific features that might determine variable activity. The only molecular mechanism associated with increased CEF activity that has so far been described involves decreased affinity for FNR in LEF (Kimata-Ariga et al., 2000). However, the amino acids responsible for this are not conserved in Fd1 sequences from either pea or Arabidopsis, and identification of the molecular determinant of Fd involvement in CEF therefore remains a future research priority

Physiological Impact of Enhanced CEF in PsFd1 Overexpressors

In previous work, $NaHSO_3$ stimulation of ATP synthesis has been found to correlate with increased growth rates (Wu et al., 2011). In this study, both CEF and LEF were stimulated by the $NaHSO_3$ treatment, while our data indicate that in *OeFd1* plants, CEF is stimulated at the expense of LEF, with the result that increased ATP/ADP ratios have no effect on the plants primary production. While some of the phenotypic features of the transformants (i.e. retarded growth and lower biomass) can be explained by the direct effects on LEF and CO_2 assimilation rates and their connection with other metabolic pathways, the variegated phenotype and the altered leaf tissue architecture (Figs. 2 and 3) deserve further attention. Leaf variegation has been attributed to faulty chloroplast biogenesis, and several Arabidopsis mutants with this phenotype (such as *immutans* and *var*) have been characterized (Aluru et al., 2006; Liu et al., 2010; Pogson and Albrecht, 2011). *Immutans* plants result from a loss-of-function mutation at *ptox*, the alternative quinone oxidase of chloroplasts, which relieves electron pressure from the PETC under conditions of excess excitation energy and preferentially in early stages of chloroplast development (Carol et al., 1999; Okegawa et al., 2010; McDonald et al., 2011). The *immutans* phenotype has been shown to be aggravated under stress conditions that induce redox imbalance in the PETC, especially at the earlier stages of development when the photosynthetic apparatus is not fully functional (Aluru et al., 2009; Rosso et al., 2009). It is noteworthy that a similar phenotype, involving growth arrest and leaf variegation, has been observed in Arabidopsis plants overexpressing the *PGR5* gene, in which CEF-PSI was constitutively elevated (Okegawa et al., 2010). Even more remarkably, the variegated *immutans* phenotype could be rescued by blocking CEF-PSI (Okegawa et al., 2010). These results indicate that there is a definite link between high turnover rates of CEF-PSI and the appearance of variegation (as in *OeFd1* plants), although the exact nature of this connection is still unknown. Within this context, variations in electron flow into the intersystem components (i.e. increased electron input driven by changes in CEF-PSI rates) might disturb regulatory processes and promote the variegation phenomenon (Foudree et al., 2010). Although it needs a deeper analysis, variegation could also contribute to the mild differences in the stoichiometry of PSII (Fig. 1) and the constitutively high values of F_0. Retrograde signals originating in the redox imbalances generated by the alternative electron partitioning might initiate reprogramming of nuclear gene expression, especially of photosynthetic genes (*PhANG*)

and also in extreme situations arrest the developmental program of the plastid (Barajas-Lopez et al., 2013).

From the analysis of TEM images, we observed that the reduced photosynthetic capacity of *OeFd1* line is associated with a decline in starch content (Fig. 3, H–J). This, in turn, leads to disappearance and/or a rearrangement of the chloroplasts located along the anticlinal cell walls of PP cells, which are exposed to the light. The movement of chloroplasts is considered a form of defense to avoid photodamage under strong light (chloroplast photorelocation movement; Kong and Wada, 2011; Tsuboi and Wada, 2011). In accordance with observations obtained in the fern *Adiantum capillus-veneris* using inhibitors of the PETC (Sugiyama and Kadota, 2011), our data suggest that this plant organelle movement probably involves crosstalk between the redox state of the PQ pool and phototropin sensors during initial light signal sensing (Kong and Wada, 2011).

In addition to chloroplast movement, the appearance of swollen thylakoids and profusion of plastoglobuli likely reflects higher osmotic pressure caused by acidification and H^+ accumulation in the lumen, as described in others mutants (Dal Bosco et al., 2004). Though the increased CEF-PSI activity in *OeFd1* lines is probably the main cause of enhanced transmembrane proton gradient and an overacidified lumen, other ions fluxes might be also participating. It has previously been reported that Ca^{2+} is transported into the thylakoid lumen by antiport with H^+ (Ettinger et al., 1999), and enhanced ΔpH in the *OeFd1* plants might also result in increased luminal Ca^{2+}, which could additionally be accompanied by uptake of Cl^- ions, exacerbating the osmotic pressure and contributing to the thylakoid swelling. The higher ATP/ADP ratio measured in these plants is also consistent with the higher H^+ gradient (Table I).

CONCLUSION

The results presented in this work complement and confirm earlier reports indicating that a division of labor does exist among Fd isoforms, which are able to differentially partition electrons between different routes of electron flow, with major (abundant) and minor (alternative) isoforms being preferentially engaged in either LEF or CEF-PSI, respectively (Hanke et al., 2008; Voss et al., 2008). Plants could take advantage of these Fd properties to modify electron partitioning between the two pathways by regulating the ratio of Fd isoforms. In line with these arguments, Voss et al. (2011) have recently shown that knockout mutation of the major isoform AtFd2 in Arabidopsis led to higher expression of nonphotosynthetic Fd (Fd3 and Fdc1), whereas AtFd1, the minor photosynthetic isoform preferentially engaged in CEF-PSI, was up-regulated only when plants were exposed to HL irradiation. Our results provide further support for the existence of a novel protective mechanism based on controlling the abundance of specific Fd isoforms. This mechanism could allow strict control of the PETC redox poise, preventing its excess reduction under adverse environmental conditions. When faced with such nonoptimal situations, the differential induction of a minor, alternative Fd isoform, such as PsFd1, which favors CEF-PSI with respect to LEF could be an adaptive mechanism to cope with excess incoming light energy. Although the molecular features that determine Fd preference for LEF or CEF-PSI have yet to be determined, it is conceivable that evolution has refined the properties of these electron carrier proteins to optimize energy use efficiency and protection under changing environments, controlling their relative abundance, affinities, and electron transfer rates.

MATERIALS AND METHODS

Generation of Tobacco Transplastomic Plants

A DNA fragment encoding mature pea (*Pisum sativum*) Fd (PsFd1; GenBank accession no. M31713) was obtained by PCR amplification using primers 5′-GGAGATATCATATGGCTTC-3′ and 5′-GATCTAGAATTAAGCAGTGAG-3′, containing *Nde*I and *Xba*I recognition sites, respectively. For chloroplast transformation, amplified DNA was digested and inserted into compatible restriction sites of plasmid pBSWutr (Wirth et al., 2006), under the control of the plastidic *rrn* and *psbA* promoters, to produce pBSWutr-PsFd1.

Tobacco (*Nicotiana tabacum* 'Petit Havana') plants were subjected to plastid transformation with pBSWUTR-PsFd1 as described by Wirth et al. (2006). After three rounds of regeneration on selective medium containing 500 μg mL^{-1} spectinomycin, several *OeFd1* plants were obtained. Homoplasmic lines were confirmed by Southern-blot analysis (Supplemental Appendix S1).

Plant Growth and Characterization

Seeds were germinated on Murashige and Skoog agar plates supplemented with 2% (w/v) Suc and, in the case of transformants, 500 μg mL^{-1} spectinomycin. After 3 weeks, seedlings were transferred to soil, watered daily, and grown at 200 μmol quanta m^{-2} s^{-1}, 25°C, and a 16/8-h photoperiod (growth chamber conditions). Unless otherwise stated, experiments were performed using 7- to 9-week-old specimens grown in soil. Protein extracts were prepared following grinding in liquid nitrogen and extraction into 50 mM Tris-HCl (pH 7.8), 5 mM $MgCl_2$, 5 mM EDTA, 5 mM dithiothreitol, and 1 mM phenylmethylsulfonyl fluoride, followed by filtration through one layer of Miracloth and centrifugation at 4,000*g* to remove debris. The presence of Fd isoforms in leaf extracts of tobacco and pea plants was determined by SDS-PAGE and immunoblot analysis with specific antisera raised against pea Fd. The levels of photosynthetic pigments were determined spectrophotometrically after ethanol extraction of leaf discs (Lichtenthaler, 1987). Other physiological measurements were determined according to Blanco et al. (2011). ATP and ADP content was determined as described by Debast et al. (2011).

Fd Purification from Mature Tobacco Leaves

Fd was purified from the mature leaves of tobacco plants 6 weeks after germination (212 g for the wild type and 145 g for OeFd1) basically as described by Buchanan and Arnon (1971), except that the initial extraction was made in 50 mM Tris-HCl, pH 7.5, and 100 mM NaCl and in the presence of 50 g preswollen polyvinyl polypyrrolidone. In addition, following first dialysis, chromatography was performed first with DEAE-cellulose, then phenyl-sepharose before a second dialysis, and finally over Q-sepharose followed by superose (all columns from GE Healthcare Europe).

Histological and Ultrastructural Analysis of Leaf Tissue

For primary fixation, 1-mm^2 sections of the second youngest fully expanded leaves were incubated for 4 h in a 2-mL dull microcentrifuge tube at

25°C in 50 mM cacodylate buffer, pH 7.2, containing 2% (v/v) glutaraldehyde and 2% (v/v) formaldehyde, followed by one wash with buffer and two washes with distilled water. For the secondary fixation, samples were transferred to 1% (w/v) OsO_4. After 1 h, they were washed three times with distilled water. Dehydration, resin embedding, and thin sectioning for light and electron microscopy were performed as described previously (Tognetti et al., 2006), except that a FEI Tecnai G2 Sphera transmission electron microscope was used for ultrastructural analysis at 120 kV.

Determination of Photosynthetic Parameters

Chlorophyll fluorescence measurements were performed using a pulse-modulated PAM-101 fluorometer with integrated PAM-103 (Walz). F_v and F_m were determined after dark adaptation of leaves for 30 min and overnight. Subsequently, leaves were exposed to 200 or 1000 μmol quanta m^{-2} s^{-1} of AL, and light-adapted values (F'_v and F'_m) were determined after 30 min of AL exposure. Photosynthetic parameters (F_0, F_v/F_m, F'_v/F'_m, Φ_{PSII}, and NPQ) were calculated as described previously (Baker, 2008). The parameters Y(PSII), Y(NO), Y(NPQ), and *qL* were obtained using a Dual-PAM-100 measuring system (Walz) according to Klughammer and Schreiber (2008).

Net CO_2 assimilation rates (A_{CO2}), ETR, and NPQ parameters were determined using LI-6400 (LI-COR) at increasing light intensities (25, 50, 100, 250, 500, 750, 1,000, 1,500, and 2,000 μmol quanta m^{-2} s^{-1}) for 3 min and 45 s for each condition.

A PAM-101 fluorometer system (Walz) was used to determine the redox state of P700 in the second attached leaves or leaf discs (1.54 cm^2). Leaves were dark adapted for at least 15 min prior to each measurement. P700 was oxidized by NIR light, and the $\Delta P700_{max}$ values were calculated from the changes in absorption at 830 and 860 nm (Voss et al., 2008).

Kinetic curves of $P700^+$ reduction in the dark were fit by a double exponential decay and the half-times were calculated as $\tau_{1/2}$= (1/k) ln2 according to Golding et al. (2004).

To evaluate PSI turnover, time courses of P700 oxidation were determined at 200 and 1000 μmol quanta m^{-2} s^{-1} of AL. Measurements were carried out on leaves that had been vacuum infiltrated (30 s) with 50 μM DBMIB as an electron blocker for PQ turnover or 100 μM MV as an electron acceptor from PSI. Control leaf discs were infiltrated with water.

Statistical Analyses

Data were analyzed using a Student's *t* test. When the normality and/or equal variance assumptions were not met, the Mann-Whitney rank sum test was used. The significance refers to statistical significance at $P < 0.05$ or $P < 0.005$.

Supplemental Data

The following materials are available in the online version of this article.

Supplemental Figure S1. Phylogenetic tree of mature plant Fds.

Supplemental Figure S2. Constructs, confirmation of homoplasmy, and phenotype of *OeFd1* lines.

Supplemental Figure S3. Fluorescence traces in *OeFd1* and wild-type plants under steady-state conditions.

Supplemental Figure S4. *OeFd1* plants have lower CO_2 assimilation activity and ETR and enhanced NPQ induction.

Supplemental Figure S5. Effect of DBMIB on P700 oxidation kinetics by NIR light.

Supplemental Figure S6. Differential P700 oxidation kinetics by AL.

Supplemental Appendix S1.

ACKNOWLEDGMENTS

We thank Dr. Néstor Carrillo and Dr. Åsa Strand for their critical reading and helpful discussion of this article.

Received November 16, 2012; accepted December 4, 2012; published December 12, 2012.

LITERATURE CITED

Aluru MR, Yu F, Fu A, Rodermel S (2006) Arabidopsis variegation mutants: new insights into chloroplast biogenesis. J Exp Bot **57:** 1871–1881

Aluru MR, Zola J, Foudree A, Rodermel SR (2009) Chloroplast photooxidation-induced transcriptome reprogramming in Arabidopsis *immutans* white leaf sectors. Plant Physiol **150:** 904–923

Baker NR (2008) Chlorophyll fluorescence: a probe of photosynthesis in vivo. Annu Rev Plant Biol **59:** 89–113

Barajas-Lopez JD, Blanco NE, Strand Å (2013) Plastid-to-nucleus communication, signals controlling the running of the plant cell. Biochim Biophys Acta **1833:** 425–437

Blanco NE, Ceccoli RD, Segretin ME, Poli HO, Voss I, Melzer M, Bravo-Almonacid FF, Scheibe R, Hajirezaei MR, Carrillo N (2011) Cyanobacterial flavodoxin complements ferredoxin deficiency in knocked-down transgenic tobacco plants. Plant J **65:** 922–935

Buchanan BB, Arnon DI (1971) Ferredoxin from photosynthetic bacteria algae and higher plants. Methods Enzymol **23:** 413–440

Burrows PA, Sazanov LA, Svab Z, Maliga P, Nixon PJ (1998) Identification of a functional respiratory complex in chloroplasts through analysis of tobacco mutants containing disrupted plastid ndh genes. EMBO J **17:** 868–876

Carol P, Stevenson D, Bisanz C, Breitenbach J, Sandmann G, Mache R, Coupland G, Kuntz M (1999) Mutations in the *Arabidopsis* gene *IMMUTANS* cause a variegated phenotype by inactivating a chloroplast terminal oxidase associated with phytoene desaturation. Plant Cell **11:** 57–68

Ceccarelli EA, Arakaki AK, Cortez N, Carrillo N (2004) Functional plasticity and catalytic efficiency in plant and bacterial ferredoxin-NADP(H) reductases. Biochim Biophys Acta **1698:** 155–165

Ceccoli RD, Blanco NE, Medina M, Carrillo N (2011) Stress response of transgenic tobacco plants expressing a cyanobacterial ferredoxin in chloroplasts. Plant Mol Biol **76:** 535–544

Ceccoli RD, Blanco NE, Segretin ME, Melzer M, Hanke GT, Scheibe R, Hajirezaei MR, Bravo-Almonacid FF, Carrillo N (2012) Flavodoxin displays dose-dependent effects on photosynthesis and stress tolerance when expressed in transgenic tobacco plants. Planta **236:** 1447–1458.

Dal Bosco C, Lezhneva L, Biehl A, Leister D, Strotmann H, Wanner G, Meurer J (2004) Inactivation of the chloroplast ATP synthase gamma subunit results in high non-photochemical fluorescence quenching and altered nuclear gene expression in *Arabidopsis thaliana*. J Biol Chem **279:** 1060–1069

DalCorso G, Pesaresi P, Masiero S, Aseeva E, Schünemann D, Finazzi G, Joliot P, Barbato R, Leister D (2008) A complex containing PGRL1 and PGR5 is involved in the switch between linear and cyclic electron flow in Arabidopsis. Cell **132:** 273–285

Daniell H, Khan MS, Allison L (2002) Milestones in chloroplast genetic engineering: an environmentally friendly era in biotechnology. Trends Plant Sci **7:** 84–91

Debast S, Nunes-Nesi A, Hajirezaei MR, Hofmann J, Sonnewald U, Fernie AR, Börnke F (2011) Altering trehalose-6-phosphate content in transgenic potato tubers affects tuber growth and alters responsiveness to hormones during sprouting. Plant Physiol **156:** 1754–1771

Dutton JE, Rogers LJ (1980) Comparative studies on the properties of two ferredoxins from *Pisum sativum* L. J Exp Bot **31:** 379–391

Edelman M, Mattoo AK (2008) D1-protein dynamics in photosystem II: the lingering enigma. Photosynth Res **98:** 609–620

Endo T, Kawase D, Sato F (2005) Stromal over-reduction by high-light stress as measured by decreases in P700 oxidation by far-red light and its physiological relevance. Plant Cell Physiol **46:** 775–781

Ettinger WF, Clear AM, Fanning KJ, Peck ML (1999) Identification of a Ca^{2+}/H^+ antiport in the plant chloroplast thylakoid membrane. Plant Physiol **119:** 1379–1386

Foudree A, Aluru M, Rodermel S (2010) PDS activity acts as a rheostat of retrograde signaling during early chloroplast biogenesis. Plant Signal Behav **5:** 1629–1632

Golding AJ, Finazzi G, Johnson GN (2004) Reduction of the thylakoid electron transport chain by stromal reductants—evidence for activation of cyclic electron transport upon dark adaptation or under drought. Planta **220:** 356–363

Gotoh E, Matsumoto M, Ogawa KI, Kobayashi Y, Tsuyama M (2010) A qualitative analysis of the regulation of cyclic electron flow around photosystem I from the post-illumination chlorophyll fluorescence

transient in Arabidopsis: a new platform for the *in vivo* investigation of the chloroplast redox state. Photosynth Res **103:** 111–123

Hanke GT, Endo T, Satoh F, Hase T (2008) Altered photosynthetic electron channelling into cyclic electron flow and nitrite assimilation in a mutant of ferredoxin:NADP(H) reductase. Plant Cell Environ **31:** 1017–1028

Hanke GT, Hase T (2008) Variable photosynthetic roles of two leaf-type ferredoxins in Arabidopsis, as revealed by RNA interference. Photochem Photobiol **84:** 1302–1309

Hanke GT, Kimata-Ariga Y, Taniguchi I, Hase T (2004) A post genomic characterization of Arabidopsis ferredoxins. Plant Physiol **134:** 255–264

Hase T, Schürmann P, Knaff DB (2006) The interaction of ferredoxin with ferredoxin-dependent enzymes. *In* JH Golbeck, ed, Photosystem I: The light-Driven Plastocyanin:Ferredoxin Oxidoreductase. Advances in Photosynthesis and Respiration, Vol 24. Springer, Dordrecht, The Netherlands, pp 477–498

Holtgrefe S, Bader KP, Horton P, Scheibe R, von Schaewen A, Backhausen JE (2003) Decreased content of leaf ferredoxin changes electron distribution and limits photosynthesis in transgenic potato plants. Plant Physiol **133:** 1768–1778

Ivanov AG, Hendrickson L, Krol M, Selstam E, Öquist G, Hurry V, Hüner NPA (2006) Digalactosyl-diacylglycerol deficiency impairs the capacity for photosynthetic intersystem electron transport and state transitions in *Arabidopsis thaliana* due to photosystem I acceptor-side limitations. Plant Cell Physiol **47:** 1146–1157

Iwai M, Takizawa K, Tokutsu R, Okamuro A, Takahashi Y, Minagawa J (2010) Isolation of the elusive supercomplex that drives cyclic electron flow in photosynthesis. Nature **464:** 1210–1213

Joliot P, Joliot A (2005) Quantification of cyclic and linear flows in plants. Proc Natl Acad Sci USA **102:** 4913–4918

Khristin MS, Akulova EA (1976) Two forms of ferredoxin in pea leaves. Biokhimiia **41:** 500–505

Kimata-Ariga Y, Matsumura T, Kada S, Fujimoto H, Fujita Y, Endo T, Mano J, Sato F, Hase T (2000) Differential electron flow around photosystem I by two C(4)-photosynthetic-cell-specific ferredoxins. EMBO J **19:** 5041–5050

Klughammer C and Schreiber U. (2008) Complementary PS II quantum yields calculated from simple fluorescence parameters measured by PAM fluorometry and the saturation pulse method. PAM Application Notes **1:** 27–35

Kofer W, Koop HU, Wanner G, Steinmüller K (1998) Mutagenesis of the genes encoding subunits A, C, H, I, J and K of the plastid NAD(P)H-plastoquinone-oxidoreductase in tobacco by polyethylene glycol-mediated plastome transformation. Mol Gen Genet **258:** 166–173

Kong SG, Wada M (2011) New insights into dynamic actin-based chloroplast photorelocation movement. Mol Plant **4:** 771–781

Kramer DM, Sacksteder CA, Cruz JA (1999) How acidic is the lumen? Photosynth Res **60:** 151–163

Lehtimäki N, Lintala M, Allahverdiyeva Y, Aro EM, Mulo P (2010) Drought stress-induced upregulation of components involved in ferredoxin-dependent cyclic electron transfer. J Plant Physiol **167:** 1018–1022

Lichtenthaler HK (1987) Chlorophylls and carotenoids: pigments of photosynthetic biomembranes. Methods Enzymol **148:** 350–382

Liu X, Yu F, Rodermel S (2010) Arabidopsis chloroplast FtsH, *var2* and suppressors of *var2* leaf variegation: a review. J Integr Plant Biol **52:** 750–761

Maliga P (2004) Plastid transformation in higher plants. Annu Rev Plant Biol **55:** 289–313

McDonald AE, Ivanov AG, Bode R, Maxwell DP, Rodermel SR, Hüner NP (2011) Flexibility in photosynthetic electron transport: the physiological role of plastoquinol terminal oxidase (PTOX). Biochim Biophys Acta **1807:** 954–967

Mulo P (2011) Chloroplast-targeted ferredoxin-NADP(+) oxidoreductase (FNR): structure, function and location. Biochim Biophys Acta **1807:** 927–934

Müller P, Li XP, Niyogi KK (2001) Non-photochemical quenching. A response to excess light energy. Plant Physiol **125:** 1558–1566

Munekage Y, Hashimoto M, Miyake C, Tomizawa K, Endo T, Tasaka M, Shikanai T (2004) Cyclic electron flow around photosystem I is essential for photosynthesis. Nature **429:** 579–582

Okegawa Y, Kobayashi Y, Shikanai T (2010) Physiological links among alternative electron transport pathways that reduce and oxidize plastoquinone in Arabidopsis. Plant J **63:** 458–468

Peltier JB, Friso G, Kalume DE, Roepstorff P, Nilsson F, Adamska I, van Wijk KJ (2000) Proteomics of the chloroplast: systematic identification and targeting analysis of lumenal and peripheral thylakoid proteins. Plant Cell **12:** 319–341

Petracek ME, Dickey LF, Nguyen TT, Gatz C, Sowinski DA, Allen GC, Thompson WF (1998) Ferredoxin-1 mRNA is destabilized by changes in photosynthetic electron transport. Proc Natl Acad Sci USA **95:** 9009–9013

Pogson BJ, Albrecht V (2011) Genetic dissection of chloroplast biogenesis and development: an overview. Plant Physiol **155:** 1545–1551

Roberts AG, Kramer DM (2001) Inhibitor "double occupancy" in the Q(o) pocket of the chloroplast cytochrome b_6f complex. Biochemistry **40:** 13407–13412

Rochaix JD (2011) Regulation of photosynthetic electron transport. Biochim Biophys Acta **1807:** 375–383

Rosso D, Bode R, Li W, Krol M, Saccon D, Wang S, Schillaci LA, Rodermel SR, Maxwell DP, Hüner NP (2009) Photosynthetic redox imbalance governs leaf sectoring in the *Arabidopsis thaliana* variegation mutants *immutans*, *spotty*, *var1*, and *var2*. Plant Cell **21:** 3473–3492

Sazanov LA, Burrows PA, Nixon PJ (1998) The chloroplast Ndh complex mediates the dark reduction of the plastoquinone pool in response to heat stress in tobacco leaves. FEBS Lett **429:** 115–118

Schürmann P, Buchanan BB (2008) The ferredoxin/thioredoxin system of oxygenic photosynthesis. Antioxid Redox Signal **10:** 1235–1274

Shikanai T (2007) Cyclic electron transport around photosystem I: genetic approaches. Annu Rev Plant Biol **58:** 199–217

Shikanai T, Endo T, Hashimoto T, Yamada Y, Asada K, Yokota A (1998) Directed disruption of the tobacco *ndhB* gene impairs cyclic electron flow around photosystem I. Proc Natl Acad Sci USA **95:** 9705–9709

Shikanai T, Munekage Y, Shimizu K, Endo T, Hashimoto T (1999) Identification and characterization of Arabidopsis mutants with reduced quenching of chlorophyll fluorescence. Plant Cell Physiol **40:** 1134–1142

Sugiyama Y, Kadota A (2011) Photosynthesis-dependent but neochrome1-independent light positioning of chloroplasts and nuclei in the fern *Adiantum capillus-veneris*. Plant Physiol **155:** 1205–1213

Tognetti VB, Palatnik JF, Fillat MF, Melzer M, Hajirezaei MR, Valle EM, Carrillo N (2006) Functional replacement of ferredoxin by a cyanobacterial flavodoxin in tobacco confers broad-range stress tolerance. Plant Cell **18:** 2035–2050

Tsuboi H, Wada M (2011) Chloroplasts can move in any direction to avoid strong light. J Plant Res **124:** 201–210

Voss I, Goss T, Murozuka E, Altmann B, McLean KJ, Rigby SE, Munro AW, Scheibe R, Hase T, Hanke GT (2011) FdC1, a novel ferredoxin protein capable of alternative electron partitioning, increases in conditions of acceptor limitation at photosystem I. J Biol Chem **286:** 50–59

Voss I, Koelmann M, Wojtera J, Holtgrefe S, Kitzmann C, Backhausen JE, Scheibe R (2008) Knockout of major leaf ferredoxin reveals new redox-regulatory adaptations in *Arabidopsis thaliana*. Physiol Plant **133:** 584–598

Wirth S, Segretin ME, Mentaberry A, Bravo-Almonacid F (2006) Accumulation of hEGF and hEGF-fusion proteins in chloroplast-transformed tobacco plants is higher in the dark than in the light. J Biotechnol **125:** 159–172

Yamamoto H, Kato H, Shinzaki Y, Horiguchi S, Shikanai T, Hase T, Endo T, Nishioka M, Makino A, Tomizawa K, et al (2006) Ferredoxin limits cyclic electron flow around PSI (CEF-PSI) in higher plants: stimulation of CEF-PSI enhances non-photochemical quenching of Chl fluorescence in transplastomic tobacco. Plant Cell Physiol **47:** 1355–1371

Yamamoto H, Peng L, Fukao Y, Shikanai T (2011) An Src homology 3 domain-like fold protein forms a ferredoxin binding site for the chloroplast NADH dehydrogenase-like complex in *Arabidopsis*. Plant Cell **23:** 1480–1493

Wu Y, Zheng F, Ma W, Han Z, Gu Q, Shen Y, Mi H (2011) Regulation of NAD(P)H dehydrogenase-dependent cyclic electron transport around PSI by $NaHSO_3$ at low concentrations in tobacco chloroplasts. Plant Cell Physiol **52:** 1734–1743